Mathematical Structures and Computational Modeling

ISSN (online): xxxx-xxxx

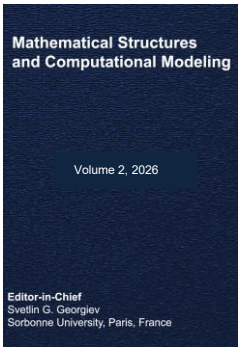

The Logistic Growth Equation: A Generalized Approach

Lucero Abril Delugo Buzaglo[1,#] and Juan E. Nápoles Valdes[1,2,*]

[1]*UNNE, FaCENA, Ave. Libertad 5450, Corrientes 3400, Argentina*
[2]*UTN-FRRE, French 414, Resistencia, Chaco 3500, Argentina*

ARTICLE INFO

Article Type: Research Article

Keywords:
Time kernels
Saturation time
Generalized derivatives
Generalized logistic growth
Adaptive numerical methods
Parametric sensitivity analysis

Timeline:
Received: February 11, 2026
Accepted: March 19, 2026
Published: April 13, 2026

Citation: Buzaglo LAD, Valdes JEN. The logistic growth equation: A generalized approach. Math Struct Comput Model. 2026; 2: 39-51.

DOI: https://doi.org/xx.xxxxx/xxxx-xxxx.2026.2.4

[#]*Student of the Bachelor's Degree in Physics.*

ABSTRACT

This work presents an exhaustive study of the generalized logistic growth equation using local fractional derivatives defined by time kernels $F(t,\alpha)$. This paper analyzes how different time structures and variations in the fractional order $\alpha \in (0,1]$ modify the saturation dynamics of the model. Four kernel families (algebraic and exponential) are considered, combined with three types of base growth rates: constant, dependent on the fractional order, and linearly increasing with time. The results, obtained through numerical integration using the adaptive RK45 method and semi-analytical solutions, reveal that the kernel choice critically determines the initial behavior of the system, potentially inducing accelerated growth or prolonged suppression (lags). Sensitivity analysis shows that the impact of the α parameter is predominant in the intermediate growth stages, although in certain exponential kernels, the differences persist even in the saturation regime. Additionally, the computational effort and saturation time are characterized, demonstrating that kernels with singularities at the origin or those that significantly delay growth impose a greater numerical demand.

AMS Subject Classification (2020): Primary 26A33, Secondary 34A08, 65L05, 92B05.

*Corresponding Author
Email: jnapoles@exa.unne.edu.ar

1. Introduction

The modeling of dynamical systems has historically relied on the integer derivative, whose local and linear nature assumes that a system's change depends exclusively on its current state. However, complex phenomena in physics, ecology, and population dynamics often exhibit behaviors that defy this simplicity, such as temporal heterogeneity, nonlinear responses to the passage of time, and structural adaptation processes.

The study of population dynamics and growth processes with saturation has been a cornerstone of mathematical biology and applied sciences since the formulation of Verhulst's model in the 19th century. The classic logistic equation, defined by the relation $\frac{dx}{dt} = rx(t)(1 - \frac{x(t)}{K})$, offers an elegant description of systems where resources are limited, balancing an initial exponential growth phase with asymptotic stabilization toward the carrying capacity K.

Nevertheless, the deterministic and local nature of the ordinary derivative is often insufficient to capture the complexity of real-world systems that exhibit memory, variable timescales, or heterogeneous media.

While the classical definitions of Caputo and Riemann-Liouville have been extensively documented (see [15]), the formalization of local derivatives in 2014 (see [8]) has allowed for a more direct interpretation of the rate of change. This derivative is called conformable, since when $\alpha \to 1$, the ordinary derivative is recovered, unlike the operators we defined in 2018, which we call non-conformable, since the above relationship does not hold (see [9, 10]).

In this scenario, generalized derivatives emerge not as a mere theoretical extension, but as a fundamental necessity for capturing the true complexity of logistic growth. The limitation of the classical derivative $\frac{dx}{dt}$ lies in its rigidity. By introducing a generalized differential operator defined through a time kernel $F(t, \alpha)$, the "geometry" of time in the differential equation is transformed. This approach allows the operator to act as a dynamic filter: depending on the functional form of the kernel (whether algebraic or exponential), the derivative can accelerate the system's perception of time or induce an inertia that faithfully models periods of latency or short memory. Thus, the logistic equation ceases to be a predetermined curve and becomes an adaptive system where the order α regulates the intensity of the interaction with the environment.

The kernel $F(t, \alpha)$ acts as a bridge between fractional calculus theory and local applications, avoiding the computational complications of non-local operators while retaining the ability to model rates of change that evolve with the process itself. In this work, the role of these derivatives is central: we analyze how the choice of kernel redefines the concept of "effective growth rate". We seek not only a numerical solution but also an understanding of how the very structure of the differential operator determines whether a system will reach saturation smoothly, abruptly, or become trapped in states of suppressed growth.

This work proposes to investigate a generalization of the logistic equation where the time derivative is replaced by a local fractional operator dependent on various families of kernels. The main focus of this study is to analyze how the interaction between the fractional order α, the kernel morphology (whether algebraic or exponential), and the nature of the growth rate $r(t)$ alters saturation times and system stability.

Throughout this study, kernels that induce everything from significant growth lags to abrupt accelerations are explored, evaluating their behavior through high-precision numerical simulations and semi-analytical analyses. This approach not only deepens the theory of nonlinear differential equations but also provides a robust framework for applications in physics, ecology, and epidemiology, where adapting the logistic model to dynamic conditions is crucial for accurately predicting equilibrium states.

2. Theoretical Framework

In 2020, a more advanced set of operators was established, surpassing those previously mentioned (see [11]), also consult [5, 21].

For a function f and a kernel $F(t,\alpha)$, the derivative of order $\alpha \in (0,1]$ is defined as:

$$N_F^{\alpha} f(t) = \lim_{\varepsilon \to 0} \frac{f(t + \varepsilon F(t,\alpha)) - f(t)}{\varepsilon}$$

This operator is local and does not necessarily satisfy Leibniz's rule in its classical form, allowing for greater flexibility in modeling complex systems.

The aforementioned local operators and others from the literature have become a useful tool in solving various modeling problems; interested readers can consult [3, 4, 12, 13].

2.1. Logistic Growth and Effective Growth Rate

Logistic growth is a classic model for describing growth processes with saturation due to limited resources and was initially proposed by Verhulst (see [17, 18]) as an alternative to Malthusian unlimited growth. In its standard form, the state variable $x(t)$ (e.g., population, biomass, or concentration) evolves according to:

$$\frac{dx}{dt} = rx(t)\left(1 - \frac{x(t)}{K}\right), \tag{1}$$

where $r > 0$ is the intrinsic growth rate and $K > 0$ is the carrying capacity or stable equilibrium. The linear term $rx(t)$ controls the initial amplification, while the factor $(1 - x/K)$ introduces negative feedback that drives saturation toward K. Readers interested in consulting classic variations of this model can consult [16].

In many contexts, however, the growth rate is not constant: it can depend on time, additional parameters, or incorporate memory effects. This type of generalization has been extensively studied within the framework of fractional calculus, particularly using local operators that preserve an interpretation close to the classical derivative and facilitate numerical implementation ([8, 6, 19]). To capture this variability, a time-dependent effective rate, denoted by $q(t)$, is considered, so that the dynamics are interpreted as time-modulated logistic growth:

$$\frac{dx}{dt} = q(t)x(t)\left(1 - \frac{x(t)}{K}\right). \tag{2}$$

In this framework, $q(t)$ summarizes in a single quantity the combined effect of the base rate and the time structure introduced by the kernel.

2.2. Temporal Kernel and Fractional Order

To explore how different temporal structures modify the dynamics, a kernel $F(t,\alpha)$ is introduced that depends on time t and a parameter $\alpha \in (0,1]$, interpreted as fractional order. In the context of generalized local fractional operators, the kernel determines the nature of the memory effect and allows conformable and non-conformable formulations to be unified within the same scheme [11, 5].

In particular, the effective rate is modeled as:

$$q(t) = \frac{r(t)}{F(t,\alpha)}, \tag{3}$$

where $r(t)$ is a base rate (potentially dependent on time or the parameter) and $F(t,\alpha)$ controls the modulation induced by the order α. This formulation is consistent with the local fractional logistic equation introduced in [1, 14] and allows for the systematic comparison of kernel families, maintaining a common logistic structure and isolating the role of time dependence.

2.3. Local Generalized Derivative and Ordinary Equivalent Form

Let $F(t,\alpha)$ be a temporal kernel with $\alpha \in (0,1]$. Within the framework of local generalized fractional derivatives, consider the operator

$$N_F^{\alpha} x(t) = F(t,\alpha)\frac{dx(t)}{dt}, \tag{4}$$

which recovers the classical derivative when $F(t,1) = 1$. Under this convention, the logistic model with local generalized derivative is written as follows:

$$N_F^{\alpha} x(t) = r(t)x(t)\left(1 - \frac{x(t)}{K}\right). \tag{5}$$

Substituting (4) into (5) yields an equivalent ordinary differential equation (ODE):

$$\frac{dx}{dt} = q(t)x(t)\left(1 - \frac{x(t)}{K}\right), \qquad q(t) = \frac{r(t)}{F(t,\alpha)}. \tag{6}$$

This equivalence allows for the numerical integration of the generalized model using standard integrators for ODEs, keeping the kernel effect within $q(t)$.

Under this formulation, different kernels produce qualitatively different behaviors:

- If $F(t,\alpha)$ induces singularities or large values near the origin, then $q(t)$ may exhibit accelerated initial growth or, conversely, be strongly suppressed.
- If $F(t,\alpha)$ grows or decays monotonically, the effective rate may shift the growth to early or intermediate times.
- In exponential kernels, small changes in α can be amplified over finite time intervals, generating persistent separations between trajectories.

In this work, three choices for the base rate are considered:

$$r(t) \in \{1,\ 2^{\alpha},\ t\}$$

which allow us to distinguish (i) growth with constant intensity, (ii) coupling explicit relationship between intensity and fractional order and (iii) a deterministic acceleration with time, as discussed in [1, 14].

2.4. Quantities of interest: sensitivity and saturation time

Conceptually, sensitivity to fractional order can be defined as:

$$\left|\frac{\partial x(t)}{\partial \alpha}\right|. \tag{7}$$

However, since this study compares a discrete set of $\alpha \in A$ values, the simulations employ an operational measure consistent with the computational procedure:

$$\Delta_{\alpha}(t) = \max_{\alpha \in \mathrm{A}} x(t;\alpha) - \min_{\alpha \in \mathrm{A}} x(t;\alpha), \qquad A = \{0.25, 0.50, 0.75\}. \tag{8}$$

This quantity quantifies the instantaneous separation between trajectories induced by fractional order and is suitable for comparing kernels under the same time frame.

Large values of $\Delta_{\alpha}(t)$ identify time windows in which fractional order strongly controls the evolution, while $\Delta_{\alpha}(t) \approx 0$ indicates regions of low parametric dependence. This quantity allows us to formalize the high sensitivity to fractional order reported in previous studies on fractional logistic models [14].

On the other hand, due to the saturating nature of the model, a quantity of interest is the *time to saturation* with respect to a fixed threshold, defined as the first time $t_{0.9}$ such that

$$x(t_{0.9}) = 0.9K, \tag{9}$$

provided that this threshold is reached within the simulation interval. This measure allows a direct comparison of the effect of the kernel $F(t,\alpha)$ and the base rate $r(t)$ on how quickly the system approaches equilibrium.

3. Numerical Considerations and Computational Procedure

Dynamics modulated by $q(t)$ can exhibit regimes with rapid time variations, such as algebraic singularities or kernel-induced abrupt transitions, which increases the numerical demands of integration. To characterize this aspect, standard metrics associated with adaptive integrators are used, such as the number of vector field evaluations ($nfev$) and the minimum effective step size (dt_{min}), widely used in the simulation of local fractional logistic models [14].

Taken together, the analysis of trajectories $x(t)$, sensitivity $\Delta_\alpha(t)$, saturation times $t_{0.9}$, and numerical effort provides a comprehensive characterization of the impact of the kernel $F(t,\alpha)$ and fractional order on a modulated logistic growth.

In all simulations, the parameters are fixed (as in the computational code): $K = 1$, $x(t_0) = x_0 = 0.5$, with $t_0 = 10^{-3}$ and final time $T = 10$. A uniform evaluation mesh of $N = 1200$ points in $[t_0, T]$ is used to visualize trajectories,

$$t_{\text{eval}} = \text{linspace}(t_0, T, 1200),$$

and fractional orders are considered:

$$\alpha \in \{0.25,\ 0.50,\ 0.75\}.$$

The choice $t_0 > 0$ avoids numerical instabilities associated with kernels exhibiting singular behavior at $t \to 0^+$ (for example, $F(t,\alpha) = t^\alpha$ induces $q(t) = t^{-\alpha}$). The equivalent ODE (6) is integrated using an explicit adaptive RK45 method with strict tolerances $\text{rtol} = 10^{-9}$ and $\text{atol} = 10^{-12}$.

Additionally, a semianalytical solution is computed from the standard logistic identity with time rate $q(t)$:

$$x(t) = \frac{x_0 K}{(K - x_0)\, exp(-p(t)) + x_0}, \qquad p(t) = \int_{t_0}^{t} q(s)ds, \tag{10}$$

where the integral $p(t)$ is numerically approximated using composite quadrature (trapezoidal rule) over t_{eval}. Comparing RK45 and (10) allows for validating numerical consistency for each combination of kernel, $r(t)$, and α.

To characterize the computational effort, metrics of the adaptive integrator are recorded: number of vector field evaluations ($nfev$), number of internal steps, and the minimum effective step size dt_{min}. These quantities are obtained by solving RK45 without imposing t_{eval} (allowing the integrator to choose its own steps).

4. Results

4.1. Kernel Analysis

4.1.1. Kernel $F(t,\alpha) = t^\alpha$

For this kernel, the effective rate takes the form

$$q(t) = r(t)t^{-\alpha},$$

which is singular at the origin and decreases with time. As shown in Figure **1**, this behavior induces very rapid growth in the early stages, especially for large values of α.

In the case $r(t) = 1$, the trajectories corresponding to $\alpha = 0.25$ and $\alpha = 0.50$ gradually converge and practically overlap at long times, while $\alpha = 0.75$ maintains a more visible separation due to a faster accumulation of $p(t)$ in the early stages.

For $r(t) = 2^{\alpha}$, the combined effect of the exponent in t and the factor 2^{α} makes the curves with $\alpha = 0.50$ and $\alpha = 0.75$ almost indistinguishable, while $\alpha = 0.25$ exhibits slower growth.

When $r(t) = t$, the trajectories intersect at intermediate times (approximately $t \approx 2$), indicating a change in the dominance of the effective rate $q(t)$; subsequently, all solutions converge to the equilibrium K.

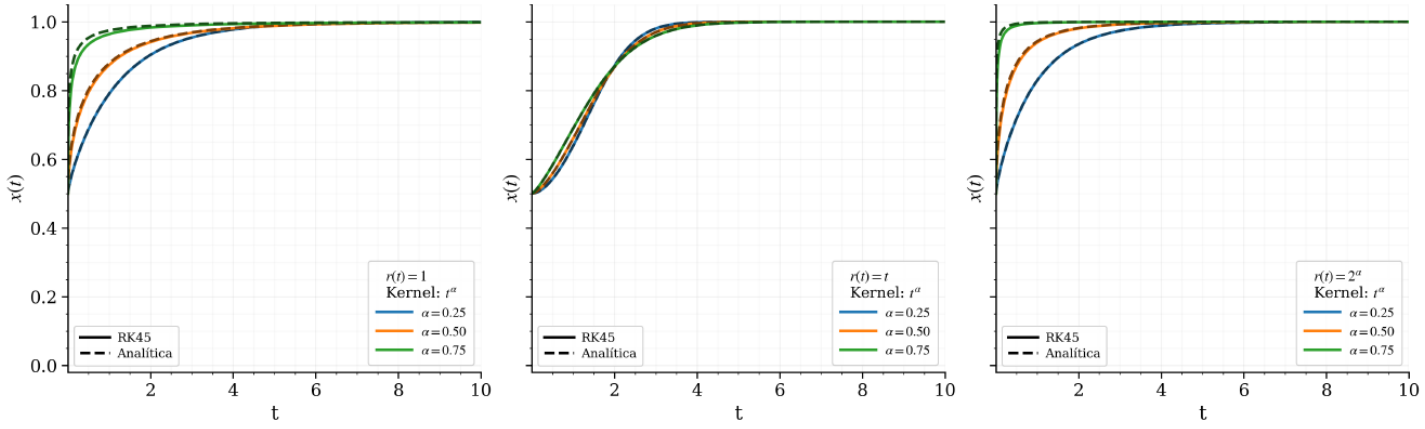

Figure 1: Analytical and numerical solutions of the local fractional logistic model for the kernel t^{α}, different fractional orders α, and growth rates $r(t)$.

4.1.2. Kernel $F(t, \alpha) = t^{-\alpha}$

In this case, we obtain

$$q(t) = r(t)t^{\alpha},$$

which vanishes at the origin and grows monotonically with time. As shown in Figure **2**, the initial growth is slow for all values of α, but it accelerates progressively.

For $r(t) = 1$, the curves intersect around $t \approx 2$, reflecting that different choices of α produce similar accumulations of $p(t)$ at that instant; subsequently, the trajectories diverge and finally converge again upon entering the logistic saturation regime.

In the case $r(t) = 2^{\alpha}$, the effective rate

$$q(t) = (2t)^{\alpha}$$

amplifies the intermediate differences, although for large times all solutions approach equilibrium again.

For $r(t) = t$, the accelerated growth of

$$q(t) = t^{1+\alpha}$$

causes all curves to quickly reach values close to K, which explains the convergence observed around $t \approx 3$.

4.1.3. Kernel $F(t, \alpha) = exp\rightleftarrows(t^{-\alpha})$

This kernel introduces a strong growth suppression effect in the early stages, since:

$$q(t) = r(t), e^{-t^{-\alpha}} \approx 0 \quad \text{for} t = 1.$$

As can be seen in Figure **3**, all trajectories begin almost completely overlapped, regardless of α, due to the almost negligible initial accumulation of $p(t)$. As t increases, the term $t^{-\alpha}$ decreases, and growth is "activated" at different times for each α, resulting in progressive separations between the curves.

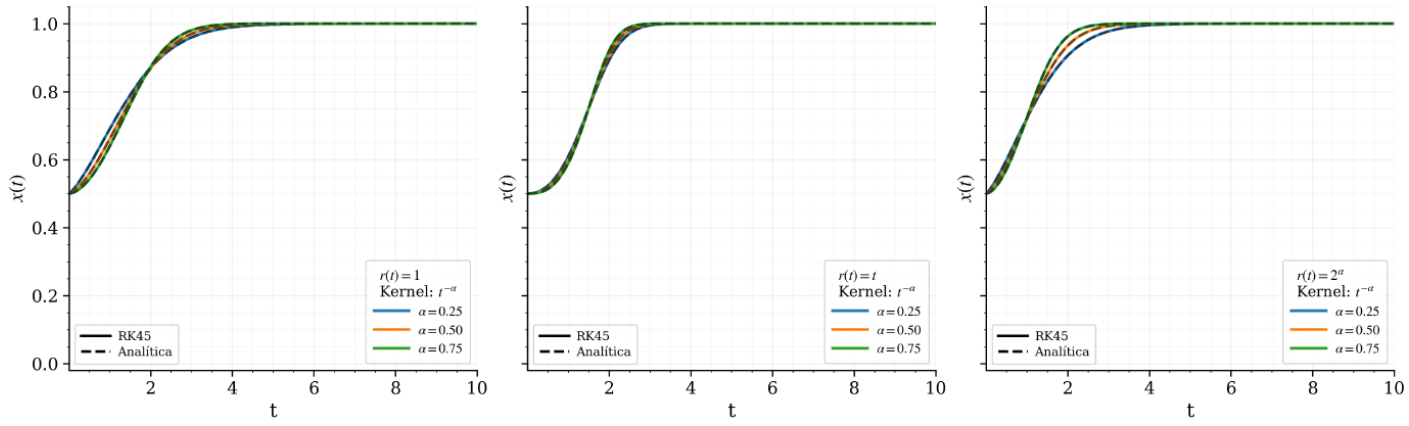

Figure 2: Analytical and numerical solutions of the local fractional logistic model for the kernel $t^{-\alpha}$, different fractional orders α, and growth rates $r(t)$.

This effect is particularly visible for $r(t) = 2^{\alpha}$ and $r(t) = t$, where the combination of a highly nonlinear kernel with a growing rate amplifies the differences at intermediate and final times.

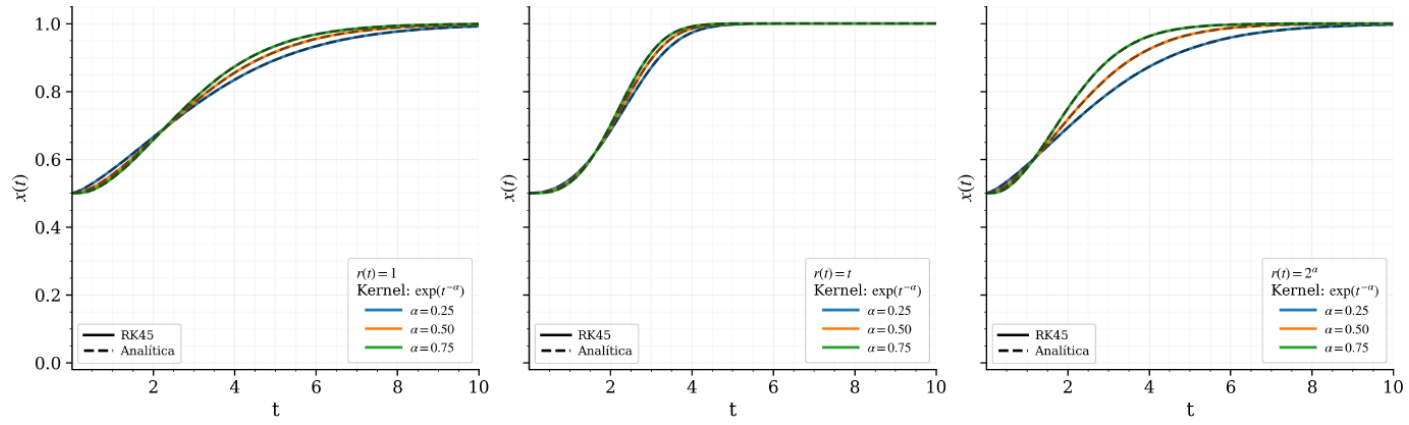

Analytical and numerical solutions of the local fractional logistic model for the kernel ($e^{t^{-\alpha}}$), different fractional orders α, and growth rates $r(t)$.

4.1.4. Kernel $F(t,\alpha) = e^{(1-\alpha)t}$

For this kernel, the effective rate is

$$q(t) = r(t)e^{-(1-\alpha)t},$$

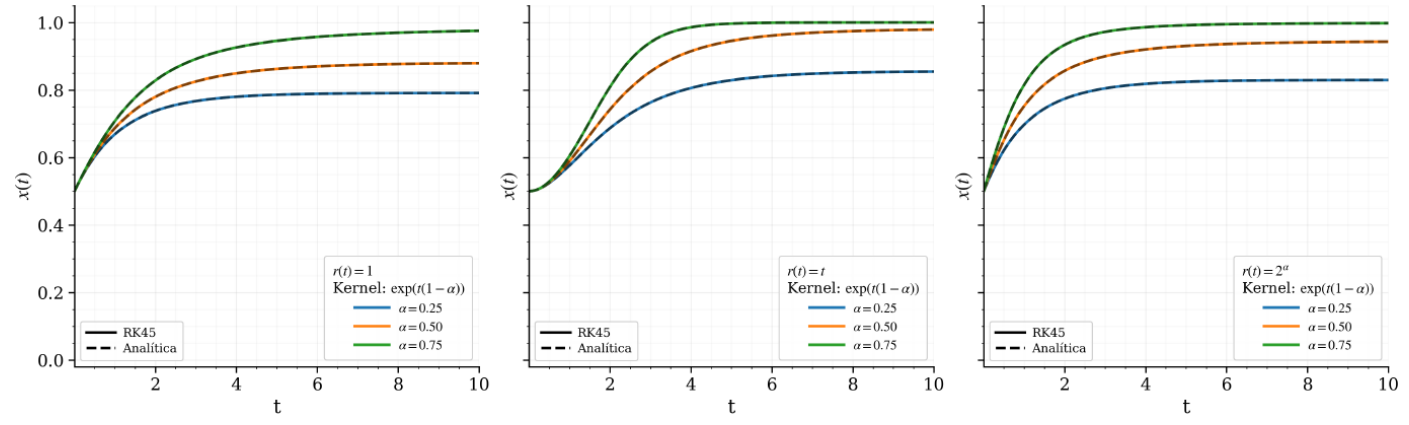

Figure 3: Analytical and numerical solutions of the local fractional logistic model for the kernel $e^{t(1-\alpha)}$, different fractional orders α, and growth rates $r(t)$.

which decays exponentially over time for $\alpha < 1$. As shown in Figure **4**, differences between values of α appear very early on: larger values of α reduce the negative exponent and, therefore, attenuate the decay of $q(t)$, resulting in faster growth.

This behavior holds qualitatively for all three choices of $r(t)$, although at different time scales. In all cases, the combined effect of the exponential kernel and the logistic term leads to smoothly diverging trajectories that slowly converge to equilibrium.

4.1.4.1. Case $r(t) = 1$

When the growth rate is constant, the differences between trajectories are due exclusively to the kernel $F(t, \alpha)$. The figures show that some kernels (such as t^{α}) concentrate growth in early times, while others (such as $t^{-\alpha}$ or $exp(\, t^{-\alpha})$) delay it.

The intersections observed between curves for different values of α indicate times at which the accumulation $p(t)$ is similar. For large times, all solutions tend towards K, and the differences decrease as the saturation regime is reached.

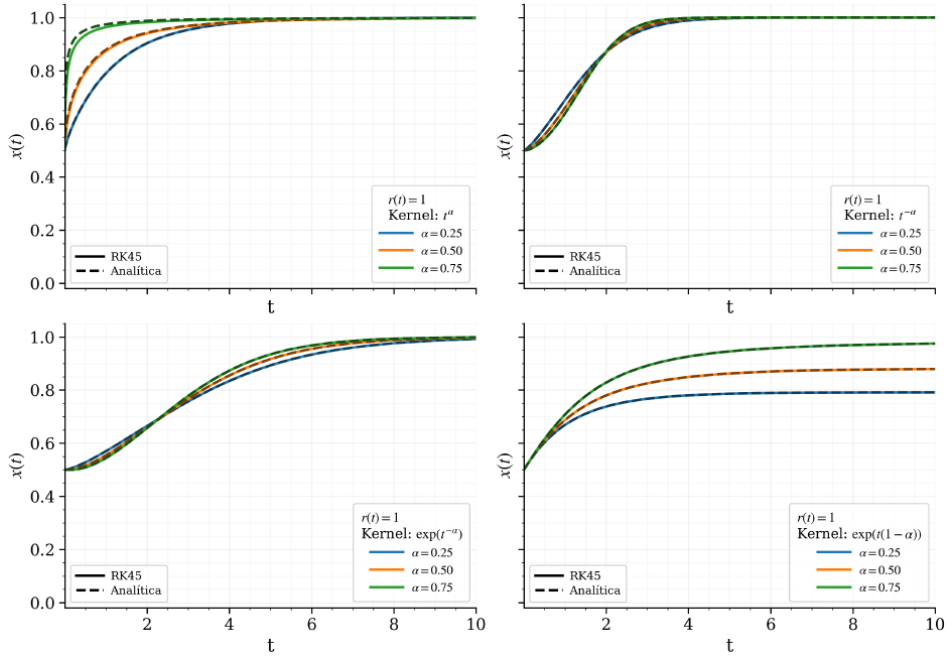

Figure 4: Analytical and numerical solutions of the local fractional logistic model for a growth rate $r(t) = 1$, different fractional orders α, and different kernels.

4.1.4.2. Case $r(t) = 2^{\alpha}$

Here, the rate depends explicitly on α, which introduces additional coupling between the kernel and the growth rate. As can be seen in the corresponding figures, this effect can either compensate for or reinforce the kernel's action: in some cases (for example, $F = t^{\alpha}$) it produces overlaps between curves for intermediate values of α, while in others (such as $F = exp(\, t^{-\alpha})$) it amplifies the separations. However, the final balance remains unchanged.

4.1.4.3. Case $r(t) = t$

When the growth rate increases linearly with time, the system exhibits richer dynamics at intermediate times. The figures show clear crossovers between trajectories for different values of α, reflecting changes in the time dominance of the effective rate $q(t)$.

However, the accelerated growth of $r(t)$ causes all solutions to quickly reach values close to K, and the differences disappear in the final regime.

4.2. Sensitivity to Fractional Order

4.2.1. Case $r(t) = 1$

For a constant growth rate, the time sensitivity to the parameter α depends strongly on the kernel considered (Fig. **5a**).

In the case of the kernel $F(t,\alpha) = t^{\alpha}$, the sensitivity exhibits a pronounced maximum at early times ($t \leq 1$), followed by a monotonic decay towards zero. This behavior indicates that the impact of α is dominant in the initial growth phase, while at later times the dynamics enter the saturation regime and the trajectories corresponding to different values of α become practically indistinguishable.

For the kernel $F(t,\alpha) = t^{-\alpha}$, the sensitivity is distributed over a wider time interval, with several moderate local maxima at $t \approx 4$, before gradually decaying towards zero at $t \approx 7$. This reflects that the effect of α is not concentrated solely at the beginning, but rather manifests itself during an intermediate growth phase.

In the case of the exponential kernel $F(t,\alpha) = exp(\, t^{-\alpha})$, the sensitivity remains relatively low at initial times and reaches a smooth maximum at intermediate times, before slowly decaying. This behavior is consistent with the presence of an initial lag in the dynamics, induced by the strong suppression of growth at $t = 1$.

Finally, for $F(t,\alpha) = e^{(1-\alpha)t}$, the sensitivity increases monotonically and stabilizes at a non-zero positive value. This indicates that, for this kernel, the differences induced by α persist even at long times and are not completely eliminated by logistic saturation.

4.2.2. Case $r(t) = 2^{\alpha}$

When the growth rate explicitly depends on the fractional order, the sensitivity to α is amplified (Fig. **5b**). In this case, the parameter α influences both the kernel and the rate $r(t)$, thus reinforcing its impact on the dynamics.

For the kernels $F(t,\alpha) = t^{\alpha}$ and $F(t,\alpha) = t^{-\alpha}$, a qualitatively similar behavior is observed: high sensitivity in the early stages, followed by a gradual decay towards zero. This suggests that, although α initially affects the growth rate, the dynamics subsequently converge towards a common regime dominated by saturation.

In contrast, the kernel $F(t,\alpha) = exp(\, t^{-\alpha})$ shows a more extended sensitivity over time, with a clearly defined intermediate maximum and slower decay. This result indicates that combining a rate dependent on α with a highly nonlinear kernel prolongs the influence of fractional order.

Finally, the kernel $F(t,\alpha) = e^{(1-\alpha)t}$ exhibits markedly different behavior: the sensitivity grows rapidly and reaches an approximately constant value for $t \approx 2$, analogous to an exponential loading process. This reveals that, in this case, the differences induced by α are persistent and do not attenuate over long periods.

4.2.3. Case $r(t) = t$

For a linear time growth rate, the sensitivity to fractional order exhibits more complex behavior at intermediate times (Fig. **6c**).

In the kernels $F(t,\alpha) = t^{\alpha}$, $F(t,\alpha) = t^{-\alpha}$, and $F(t,\alpha) = exp(\, t^{-\alpha})$, the sensitivity is concentrated mainly in the interval $0 < t \approx 4$, where well-defined maxima appear associated with changes in the dominance of the effective growth rate. Subsequently, $\Delta_{\alpha}(t)$ rapidly decays towards zero for $t \approx 5$, indicating that the influence of α becomes negligible once the system enters the accelerated saturation regime induced by $r(t) = t$.

In contrast, the kernel $F(t,\alpha) = e^{(1-\alpha)t}$ shows rapid and sustained sensitivity growth, reaching significantly higher values than those observed for the other kernels. This result highlights that the combination of an increasing growth rate and an exponential kernel significantly amplifies the impact of fractional order. This generates persistent differences between trajectories corresponding to different values of α.

4.3. Numerical Effort

4.3.1. Case $r(t) = 1$

For a constant growth rate, the numerical effort depends primarily on the kernel and, to a lesser extent, on the fractional order α (Fig. **5a**).

The kernel $F(t,\alpha) = t^{\alpha}$ requires a large number of vector field evaluations, on the order of $nfev \approx 500$, with moderate variations between different values of α. This behavior is consistent with the presence of an algebraic singularity in the effective rate $q(t) = t^{-\alpha}$, which necessitates sustained refinement of the time step in early times.

The kernel $F(t,\alpha) = t^{-\alpha}$ exhibits the greatest computational effort within this group, reaching values close to the observed maximum ($nfev \approx 550$–580). This indicates that, although the minimum step size is not extremely small, the delayed dynamics at the beginning and the subsequent acceleration force the integrator to perform a large number of adaptive steps.

For the kernel $F(t,\alpha) = exp(t^{-\alpha})$, the numerical effort is intermediate, with $nfev$ values clearly increasing as α increases. This result reflects that, although growth is strongly suppressed at the beginning, the transition to the active phase is extended over time and requires a significant number of evaluations.

Finally, the kernel $F(t,\alpha) = e^{(1-\alpha)t}$ is the least computationally expensive for $r(t) = 1$, especially for small values of α. However, there is a noticeable increase in $nfev$ when going from $\alpha = 0.25$ to $\alpha = 0.75$, which indicates that the persistence of dynamic differences over long times increases the total effort of the integrator.

4.3.2. Case $r(t) = 2^{\alpha}$

When the growth rate explicitly depends on the fractional order, the numerical effort generally increases (Fig. **5b**), reflecting the combined effect of $r(t)$ and the kernel.

In this case, all kernels reach $nfev$ values on the order of 550â€“600. For $F(t,\alpha) = t^{\alpha}$, the number of evaluations grows systematically with α, increasing from approximately $nfev \approx 500$ for $\alpha = 0.25$ to values close to 600 for $\alpha = 0.75$. This increase confirms that the growth boost induced by 2^{α} amplifies the time complexity of the dynamics.

The kernel $F(t,\alpha) = t^{-\alpha}$ is the most computationally demanding in this regime, reaching the maximum values of $nfev$. This agrees with the numerical hardness results, where relatively small minimum steps are observed over extended time intervals.

For $F(t,\alpha) = exp(t^{-\alpha})$, the numerical effort also increases with α, although more gradually. In this case, the cost is dominated by the duration of the transient regime rather than by the presence of an extreme local singularity.

In the case $F(t,\alpha) = e^{(1-\alpha)t}$ remains the least costly, although it shows a clear increase in $nfev$ as α increases, confirming that persistent differences between trajectories also impact the overall cost.

For a linear growth rate, the numerical effort reaches the highest values among the three cases considered (Fig. **5c**), indicating that the time acceleration of the dynamics significantly increases the computational cost.

The kernels $F(t,\alpha) = t^{\alpha}$ and $F(t,\alpha) = exp(t^{-\alpha})$ exhibit relatively stable $nfev$ values, on the order of 500-550, with a moderate dependence on α. In these cases, the increase in the growth rate tends to concentrate the dynamics in intermediate time intervals, without generating sustained extreme hardness.

In contrast, the kernel $F(t,\alpha) = t^{-\alpha}$ shows a pronounced increase in numerical effort with α, reaching values close to $nfev \approx 900$ for $\alpha = 0.75$. This result indicates that the combination of an initially delayed growth and a growing rate over time creates a particularly demanding dynamic for the integrator.

Lastly, the kernel $F(t,\alpha) = e^{(1-\alpha)t}$ again exhibits the lowest $nfev$ values, although with a noticeable increase as α increases. This confirms that, even though the local hardness is not extreme, the temporal persistence of the sensitivity induces an additional cumulative cost.

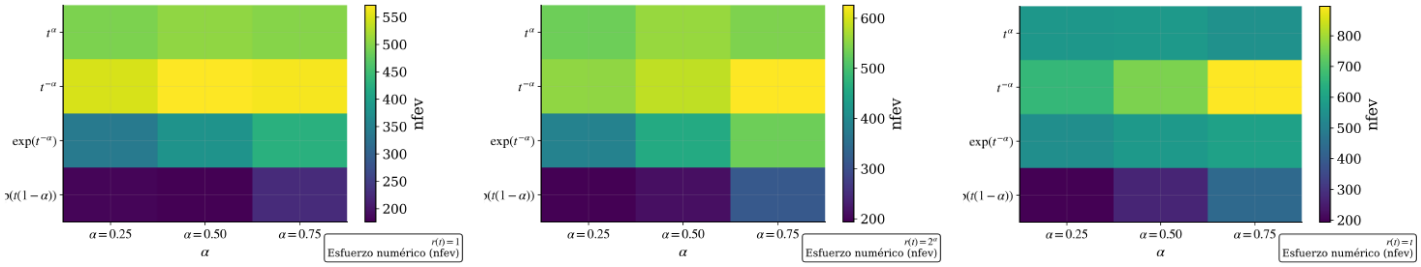

(a) (b) (c)

Figure 5: Numerical effort according to fractional order for different kernels and the same growth rate.

4.4. Saturation Time Analysis

4.4.1. Saturation Time for $r(t) = 1$

For a constant growth rate, the saturation time depends significantly on the kernel and the fractional order α (Fig. **6a**). Please correc

In the case of the kernel $F(t,\alpha) = t^{\alpha}$, it can be observed that $t_{0.9}$ increases as α increases. This indicates that, although the initial growth may be rapid for certain values of α, the cumulative effect of the kernel delays the arrival at the regime close to the load capacity.

For the kernel $F(t,\alpha) = t^{-\alpha}$, the saturation time remains at intermediate values and shows a weak dependence on α. This behavior reflects a balance between the initial delay and the subsequent acceleration of growth.

The kernel $F(t,\alpha) = exp(\,t^{-\alpha})$ exhibits the highest values of $t_{0.9}$ among the kernels considered, confirming that strong early growth suppression significantly delays saturation. In this case, the system remains in a slow growth regime for extended periods.

Ultimately, for $F(t,\alpha) = e^{(1-\alpha)t}$, it is observed that for small values of α, the solution does not reach the $0.9K$ threshold within the simulated interval, as reflected in the blank regions of the map. This indicates that the kernel induces persistent growth damping that strongly delays saturation.

4.4.2. Time to Saturation for $r(t) = 2^{\alpha}$

When the growth rate explicitly depends on the fractional order, the time to saturation is significantly modified (Fig. **6b**).

For the kernel $F(t,\alpha) = t^{\alpha}$, $t_{0.9}$ decreases as α increases, reflecting the accelerating effect of the rate $r(t) = 2^{\alpha}$. In this case, larger values of α lead to earlier saturation.

In contrast, the kernel $F(t,\alpha) = t^{-\alpha}$ shows relatively large values of $t_{0.9}$ and a smooth dependence on α, indicating that the kernel-induced delay partially compensates for the increased growth rate.

The kernel $F(t,\alpha) = exp(\,t^{-\alpha})$ again exhibits the longest saturation times, especially for small values of α, where regions are even observed in which the system does not reach the threshold $0.9K$ within the considered interval.

For $F(t,\alpha) = e^{(1-\alpha)t}$, a mixed pattern is observed: for small values of α, the growth is so damped that $t_{0.9}$ is undefined, while for larger values of α, saturation occurs in finite but relatively long times.

4.4.3. Time to Saturation for $r(t) = t$

For a growth rate that increases linearly with time, the time to saturation exhibits a different structure (Fig. **6c**).

In the kernels $F(t,\alpha) = t^{\alpha}$ and $F(t,\alpha) = t^{-\alpha}$, $t_{0.9}$ takes moderate values and shows a smooth variation with α. The accelerated growth of $r(t)$ favors an early arrival at the state close to the load capacity.

In the case of the kernel $F(t,\alpha) = exp(\,t^{-\alpha})$, the time to saturation is considerably longer, confirming that the initial delay induced by the kernel is not completely compensated by the growth rate $r(t)$.

Finally, for $F(t,\alpha) = e^{(1-\alpha)t}$, blank regions are observed for small values of α, indicating that the system does not reach saturation within the considered interval. For larger values of α, the growth becomes sufficient to reach the threshold, although over relatively long periods.

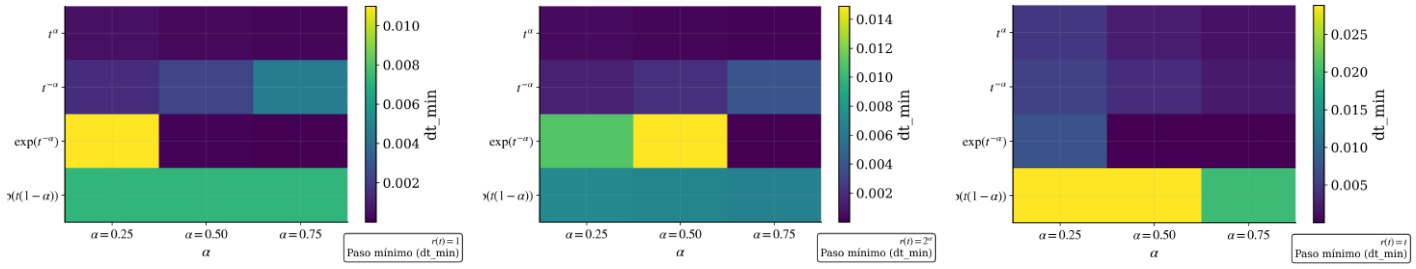

(a) (b) (c)

Figure 6: Saturation time according to fractional order for different kernels and the same growth rate.

5. Conclusions

This study has demonstrated that the generalization of the logistic equation using local derivatives with time kernels $F(t,\alpha)$ is not merely a formal extension, but a superior conceptual framework for modeling complex growth processes. Through the analysis of various families of kernels and growth rates, the following key conclusions have been reached:

1. **Versatility and Adaptability of the Differential Operator:** The main advantage of generalized derivatives lies in their ability to act as "modulators of time dynamics." While the classical derivative imposes a uniform progression, the kernels analyzed allow for capturing inertia phenomena (lag effect) or sudden acceleration simply by adjusting the parameter α and the functional morphology of the kernel. This gives the model a flexibility that integer-order differential equations cannot offer without adding excessive structural complexity.
2. **Critical Influence of Kernel Structure:** Exponential kernels, such as $F(t,\alpha) = exp(\,t^{-\alpha})$, have been shown to have a unique ability to delay the initial growth phase, modeling biological or physical systems that require a "warm-up" period. Conversely, algebraic kernels allow for a smoother transition to saturation. This distinction is crucial for model selection in real-world applications, where the initial phase of a process can be as important as its equilibrium state.
3. **Independence and Sensitivity of Parameters:** Sensitivity analysis revealed that the fractional order α has a dominant impact on the saturation time ($t_{0.9}$), but its effect is closely linked to the nature of the growth rate $r(t)$. It was observed that a linearly increasing growth rate can compensate for the damping induced by certain kernels, suggesting that the interaction between the differential operator and the source term is key to the system's stability.
4. **Computational Efficiency and Numerical Robustness:** Despite the sophistication of generalized operators, the use of local derivatives allows for efficient numerical implementation using adaptive methods such as RK45. This represents a competitive advantage over non-local fractional derivatives (such as Caputo

or Riemann-Liouville), as it yields similar dynamic richness without the high computational cost of storing the complete system history (long memory).

5. **Projection and Applicability:** In conclusion, the proposed generalized derivatives approach provides a robust tool for scientists and engineers. The ability to adjust the system's response through the kernel $F(t, \alpha)$ allows the logistic model to adapt to a vast range of scenarios, from the diffusion of technological innovations to the spread of epidemics in heterogeneous media, where boundary conditions and response times change dynamically.

All of the above opens up new lines of research using other local operators defined in recent years, such as those defined in [2, 7, 20].

References

[1] Abreu Blaya R, Fleitas A, Nápoles Valdés JE, Reyes R, Rodríguez JM, Sigarreta JM. On the conformable fractional logistic models. Math Methods Appl Sci. 2020;43:4156–67.

[2] Castillo RE, Nápoles Valdes JE, Chaparro H. Omega derivative. Gulf J Math. 2024;16(1):55–67. doi: 10.56947/gjom.v16i1.1430

[3] Chatzarakis GE, Nápoles Valdes JE. Continuability of Liénard's type system with generalized local derivative. Discontinuity Nonlinearity Complex. 2023;12(01):1–11.

[4] Fleitas A, Méndez-Bermúdez JA, Nápoles Valdes JE, Sigarreta Almira JM. On fractional Liénard-type systems. Rev Mex Fís. 2019;65(6):618–25.

[5] Fleitas A, Nápoles Valdés JE, Rodríguez JM, Sigarreta JM. Note on the generalized conformable derivative. Rev la UMA. 2021;62(2):443–57.

[6] Guzmán PM, Langton G, Lugo LM, Medina J, Nápoles Valdé JE. A new definition of a fractional derivative of local type. J Math Anal. 2018;9(2):88–98.

[7] Guzmán PM, Nápoles Valdes JE, Vivas-Cortez M. A new generalized derivative and related properties. Appl Math Inf Sci. 2024;18(5):923–32. doi: 10.18576/amis/180501

[8] Khalil R, Al Horani M, Yousef A, Sababheh M. A new definition of fractional derivative. J Comput Appl Math. 2014;264:65–70.

[9] Martínez F, Nápoles Valdes JE. Towards a non-conformable fractional calculus of n-variables. J Math Appl. 2020;43(1):87–98.

[10] Nápoles Valdes JE, Guzmán PM, Lugo Motta Bittencourt LM. Some new results on nonconformable fractional calculus. Adv Dyn Syst Appl. 2018;13(2):167–75.

[11] Nápoles Valdés JE, Guzmán PM, Lugo LM, Kashuri A. The local generalized derivative and Mittag-Leffler function. Sigma J Eng Nat Sci. 2020;38(2):1007–17.

[12] Nápoles Valdes JE, Brisa AR, Lautaro S, Moragues SMAF. Numerical simulation of local generalized derivative for a harmonic oscillator. J Phys Appl Mech. 2022;1(1):1003.

[13] Nápoles Valdes JE, Roa PM. Numerical simulations in a generalized Liénard's type system. Ann Math Phys. 2023;6(2):187–95. doi: 10.17352/amp.000101

[14] Nápoles Valdés JE, Torres MO. Numerical simulation of the local generalized derivative for the fractional logistic model. J Math Artif Intell. 2025;1(1):11–22.

[15] Podlubny I. Fractional differential equations. San Diego: Academic Press; 1998.

[16] Tsoularis A, Wallace J. Analysis of logistic growth models. Math Biosci. 2002;179(1):21–55.

[17] Verhulst PF. Notice sur la loi que la population suit dans son accroissement. Corresp Math Phys. 1838;10:113–21.

[18] Verhulst PF. Recherches mathématiques sur la loi d'accroissement de la population. Nouv Mém Acad R Sci Belles-Lett Brux. 1845;18:1–42.

[19] Vivas-Cortez M, Guzmán PM, Lugo LM, Nápoles Valdés JE. Fractional calculus: historical notes. Rev MATUA. 2021;8(2):1–13.

[20] Vivas-Cortez M, Lugo LM, Nápoles Valdes JE, Samei ME. A multi-index generalized derivative; some introductory notes. Appl Math Inf Sci. 2022;16(6):883–90.

[21] Zhao D, Luo M. General conformable fractional derivative and its physical interpretation. Calcolo. 2017;54:903–17. doi: 10.1007/s10092-017-0213-8